

## Enhancement of the electron-irradiation-induced amorphization of $Zr_2Ni$ and $Zr_3Al$ by hydrogen

D. K. Tappin, I. M. Robertson, and H. K. Birnbaum

*Department of Materials Science and Engineering and the Frederick Seitz Materials Research Laboratory,  
University of Illinois, Urbana, Illinois 61801*

(Received 1 July 1994)

An examination of the effect of interstitial hydrogen on electron-irradiation-induced amorphization of  $Zr_2Ni$  and  $Zr_3Al$  has been carried out. Irradiations were performed at a variety of temperatures on hydrogen-free and on electrochemically or gaseously charged specimens. An average hydrogen concentration of a few percent was found to substantially alter the amorphization process. In the presence of hydrogen, the electron dose required to achieve amorphization of the  $Zr_3Al$  alloy was significantly reduced. For  $Zr_2Ni$  it was found that the upper temperature limit, below which complete amorphization occurred, was substantially increased. From the experimental results obtained, it is proposed that the role of hydrogen is primarily to increase the stability of the defective structure rather than to increase, by secondary displacements, the number of Frenkel pairs.

### INTRODUCTION

Recent work by Meng, Koike, Okamoto, and Rehn<sup>1</sup> on the amorphization of  $Zr_3Al$  by electron irradiation has shown that the presence of hydrogen can reduce the electron dose required for complete amorphization of the crystalline lattice.  $Zr_3Al$  is known to be amorphized by interstitial hydrogen,<sup>2</sup> and the primary mechanism for the enhancement of the electron-irradiation-induced amorphization process was suggested to be a reduction in the free-energy difference between the amorphous and crystalline material due to hydrogen. In the absence of hydrogen,  $Zr_3Al$  is difficult to amorphize by electron irradiation. The work of Koike, Okamoto, Rehn, and Meshii<sup>3</sup> shows that, at 10 K, 26 displacements per atom (dpa) produces approximately 90% amorphization. At this displacement level, irradiation at a temperature of 295 K induces partial amorphization, and a rhombohedral distortion of the crystalline lattice. Defects, typical of radiation damage in elemental metals, were observed at all the temperatures examined and the average size of the defects was reported to increase as the irradiation temperature was increased. The formation of such defects is not normally observed in metals which undergo complete amorphization.

The "critical temperature," which we define as the upper temperature for electron-irradiation-induced amorphization to occur, is not known in the  $Zr_3Al$  system. By contrast,  $Zr_2Ni$ , in the absence of hydrogen, is known to amorphize relatively easily and the variation in the electron dose to amorphization with irradiation temperature has been well characterized.<sup>4</sup> This system has, therefore, been examined to investigate the enhancement of the electron-irradiation-induced amorphization by hydrogen, and to determine the effect of hydrogen on the critical temperature. Further data on the influence of hydrogen on the electron-induced amorphization behavior of the  $Zr_3Al$  system are also presented.

### EXPERIMENTAL METHODS

Specimens of  $Zr_2Ni$  were prepared by arc-melting high-purity Ni with Zr sponge or 99% Zr rod under an argon atmosphere of 20 Pa. The arc-melting system was evacuated to a level of  $1 \times 10^{-4}$  Pa prior to repeated flushing by high-purity Ar to reduce the partial pressure of contaminant gases. Specimens were overturned and remelted a minimum of four times to ensure thorough mixing of the components. The alloys were homogenized at 1273 K for 48 h under a vacuum of  $1 \times 10^{-5}$  Pa. Specimens of well-ordered  $Zr_3Al$  were supplied by Dr. L. E. Rehn of Argonne National Laboratory.

The structures of the  $Zr_2Ni$  and  $Zr_3Al$  specimens were confirmed using a Rigaku D-Max x-ray diffractometer. The  $Zr_2Ni$  specimens were essentially single phase, with all the  $2\theta$  peaks corresponding to the C16 structure.<sup>5,6</sup> The  $Zr_3Al$  specimen showed a number of diffraction peaks corresponding to  $Zr_2Al$ .

Transmission electron microscopy (TEM) specimens, in the form of 3 mm disks, were punched ( $Zr_3Al$ ) or spark machined ( $Zr_2Ni$ ) from 250  $\mu m$  slices of the alloys. The disks were mechanically polished to 9  $\mu m$  finish prior to jet polishing in a Tenupol III. Specimens of  $Zr_2Ni$  were prepared using a variety of standard acidic electropolishing solutions. In addition, to ascertain that hydrogen absorption during electropolishing did not influence the amorphization behavior of the non-hydrogen-charged specimens, a water-free 0.5M solution of  $Mg(ClO_4)_2$  in methanol<sup>7</sup> was used. Similar results were obtained for all the polishes used, indicating that an insignificant concentration of hydrogen was introduced during electropolishing. Specimens were stored under a vacuum of  $10^{-5}$  Pa prior to irradiation.

Hydrogen was introduced into the  $Zr_2Ni$  alloys by cathodic charging for between 60 and 300 s in a 10% solution of phosphoric acid ( $H_3PO_4$ ) in deionized water at an applied voltage of 3 V. Two different stainless steel

anodes were used during the cathodic charging procedure: a large ( $\sim 7$  cm diameter) cylindrical anode and a smaller plate anode ( $\sim 5$  cm<sup>2</sup>). The shape of the anode has a significant influence on the distribution of hydrogen within the specimen. The plate anode will introduce hydrogen predominantly on one side of the TEM disk; that which faces the anode. A cylindrical anode, by contrast, will introduce hydrogen throughout the surface of the specimen. At room temperature little hydrogen is lost from the specimen<sup>8</sup> and it is probable that minimal diffusion of the hydrogen occurs in the time frame of the experiments (2–3 days). An additional specimen was also prepared by gas-phase-charging an unpolished Zr<sub>2</sub>Ni disk in 1 atm of hydrogen at 323 K for approximately four weeks.

By contrast to the Zr<sub>2</sub>Ni samples, a significant concentration of hydrogen was introduced into the Zr<sub>3</sub>Al specimens during electropolishing in a solution of 5% perchloric acid in methanol at room temperature. Nominally hydrogen-free samples were prepared using the same solution at temperatures of  $\sim 220$  K.

The hydrogen content of the alloys was determined by thermal desorption of the hydrogen in a rf furnace and analysis of the desorbed gases in a Hewlett-Packard 5890A gas chromatograph. Analysis of uncharged specimens of Zr<sub>2</sub>Ni, polished using an acidic solution, confirmed that an insignificant amount of hydrogen ( $< 0.4$  at. % H) was absorbed during electropolishing. Cathodic charging introduced between 2 and 8 at. % H. The overall hydrogen content of the Zr<sub>2</sub>Ni alloys was similar for the specimens charged with either the cylindrical or the plate cathode. Thus the primary difference between the two specimens was the distribution of hydrogen, rather than the hydrogen content. The specimen which had undergone gaseous charging exhibited an equivalent hydrogen concentration to the cathodically charged specimens.

A significant concentration of hydrogen (1.5 at. % H) was introduced in the Zr<sub>3</sub>Al by electropolishing at room temperature. The distribution of the hydrogen in this case is expected to be similar to that for the Zr<sub>2</sub>Ni specimens charged using a cylindrical anode as the electropolishing occurred on both faces of the 3 mm disk.

Electron irradiations were performed in the Argonne HVEM Tandem facility<sup>9</sup> at an accelerating voltage of 1 MeV using a liquid-helium-cooled double-tilt stage. This permitted the temperature to be varied in the range 10–300 K. A fully focused electron beam was used for the irradiations, with the dose rate being varied by altering the size of the condenser aperture. The dose rate could be varied between  $1 \times 10^{19}$  and  $\sim 1 \times 10^{20}$  electrons cm<sup>-2</sup>s<sup>-1</sup> using this technique. The beam currents corresponding to these dose rates are approximately 50 and 500 nA, respectively. The increase in the sample temperature due to beam heating was calculated according to Fisher's<sup>10</sup> formulation and was  $< 5$  degrees for a beam current of 50 nA and about 45 degrees for a beam current of 500 nA. The same electron-beam currents were used for irradiations of the hydrogen-charged and hydrogen-free materials.

The amorphization process was monitored by examin-

ing the specimen area within the central region of the electron beam. Photographs of the diffraction patterns were taken with the condenser overfocused. It was found that, in some cases, the images showed weak diffraction spots or intensity variations in the amorphous ring which were not visible on the fluorescent screen of the microscope. Photographically recorded diffraction pattern images were, therefore, used exclusively to determine whether the amorphization reaction was complete.

Formation of a polycrystalline phase during ambient-temperature irradiation of the Zr<sub>2</sub>Ni alloys was also monitored at higher resolution by irradiating the specimens, at room temperature, with 400 keV electrons in a JEOL 4000 EX TEM fitted with an environmental cell.<sup>11</sup> No quantitative dose information was, however, available.

## EXPERIMENTAL RESULTS

### A. Zr<sub>2</sub>Ni

The variation in the electron dose required for amorphization with irradiation temperature for the hydrogen-free Zr<sub>2</sub>Ni specimens is shown as open squares in Fig. 1. As shown in this figure, the minimum electron dose required for complete amorphization was about  $7.6 \times 10^{21}$  electrons cm<sup>-2</sup> and is essentially independent of temperature until a temperature of  $\sim 100$  K is reached. In this low-temperature range irradiations which were performed in thicker regions of the specimen required a larger dose to completely transform to the amorphous state, or did not completely transform at the minimum dose (e.g., at 48 K) (an incomplete amorphization is shown as a diamond in Fig. 1). In this temperature range, the effect of the dose rate on the total dose to produce amorphization was small.

As the irradiation temperature was increased (100–160 K) a small, but consistent, increase in the dose required for complete amorphization was observed. At 160 K the

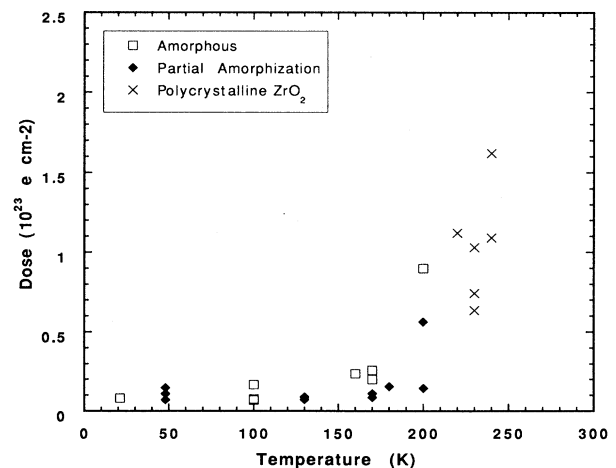


FIG. 1. The variation in the electron dose (electrons cm<sup>-2</sup>) required for complete amorphization (□), partial amorphization (◆), and formation of a polycrystalline surface ZrO<sub>2</sub> (×) with irradiation temperature for hydrogen-free Zr<sub>2</sub>Ni.

minimum dose for amorphization was  $\sim 2.5 \times 10^{22}$  electrons  $\text{cm}^{-2}$ . Such effects could not be attributed to changes in the foil thickness. Above 170 K, the electron dose rate was increased from  $1.5 \times 10^{19}$  to  $5 \times 10^{19}$  electrons  $\text{cm}^{-2} \text{s}^{-1}$  to reduce the time required for amorphization. At a temperature of 200 K, a significant increase in the electron dose required for complete amorphization was observed, with the value being  $\sim 9 \times 10^{22}$  electrons  $\text{cm}^{-2}$ . This temperature appears to mark the "critical temperature" for electron-irradiation-induced amorphization in hydrogen-free  $\text{Zr}_2\text{Ni}$  as it corresponds to the temperature above which no amorphization was observed, even for electron doses as high as  $1.5 \times 10^{24}$  electrons  $\text{cm}^{-2}$  at 220 K.

Above 200 K, irradiation of the alloy induced the formation of a polycrystalline, cubic,  $\text{ZrO}_2$  oxide phase at the surface of the specimen, shown as the  $\times$  in Fig. 1. The typical microstructure induced by the formation of  $\text{ZrO}_2$  is shown for a 400 keV electron irradiation at 300 K in Fig. 2. The larger oxide particles appear to form from the coalescence of smaller adjacent particles, the boundaries of which may still be seen in some of the larger microcrystals. The grain boundary, present in the upper region of the figure (arrowed), does not appear to influence the transformation, with no evidence for enhanced or decreased production of the oxide phase. This suggests that the partial pressure of oxygen present within the HVEM (or JEOL 4000 TEM) during electron irradiation was responsible for the behavior, rather than oxygen contamination within the specimen, which would influence the formation of oxide at the grain boundary. Further evidence for this was obtained by subjecting the specimen to a higher level of vacuum (using the environ-

mental cell facility<sup>11</sup> of the TEM) and performing electron irradiations at 400 kV. In this case no oxide formation was observed. Additionally, no evidence for an oxide or for the metastable  $E9_3$  phase, which is stabilized by oxygen in many C16 alloys,<sup>12</sup> was found in the x-ray diffraction data for the unirradiated specimens.

Data shown as open circles in Fig. 3 show the variation in the dose to complete amorphization with irradiation temperature for the hydrogen-charged  $\text{Zr}_2\text{Ni}$ . The data shown were obtained from specimens which had undergone cathodic charging using a cylindrical anode or had undergone gas-phase charging. No amorphization due to the presence of hydrogen was detected in the diffraction patterns prior to irradiation. For comparison, the amorphization data obtained for the hydrogen-free material are also shown (as open squares) in the figure. It can be seen that, at temperatures approaching, and slightly above, the critical temperature for amorphization in the hydrogen-free material (200 K), the hydrogen-doped alloys exhibit complete amorphization at generally lower dose levels than those required for hydrogen-free  $\text{Zr}_2\text{Ni}$ . In some cases, the electron dose required for complete amorphization is as low as that observed for irradiations performed at temperatures of less than 100 K in the hydrogen-free material. Complete amorphization of the hydrogen-doped material was observed at temperatures up to 230 K with partial amorphization (in most cases very close to complete amorphization) occurring at temperatures as high as 260 K. In these experiments the incidence of the polycrystalline oxide phase was significantly reduced and, as shown in Fig. 3, the presence of this phase does not *a priori* prevent the formation of the amorphous phase. The increase in the "critical

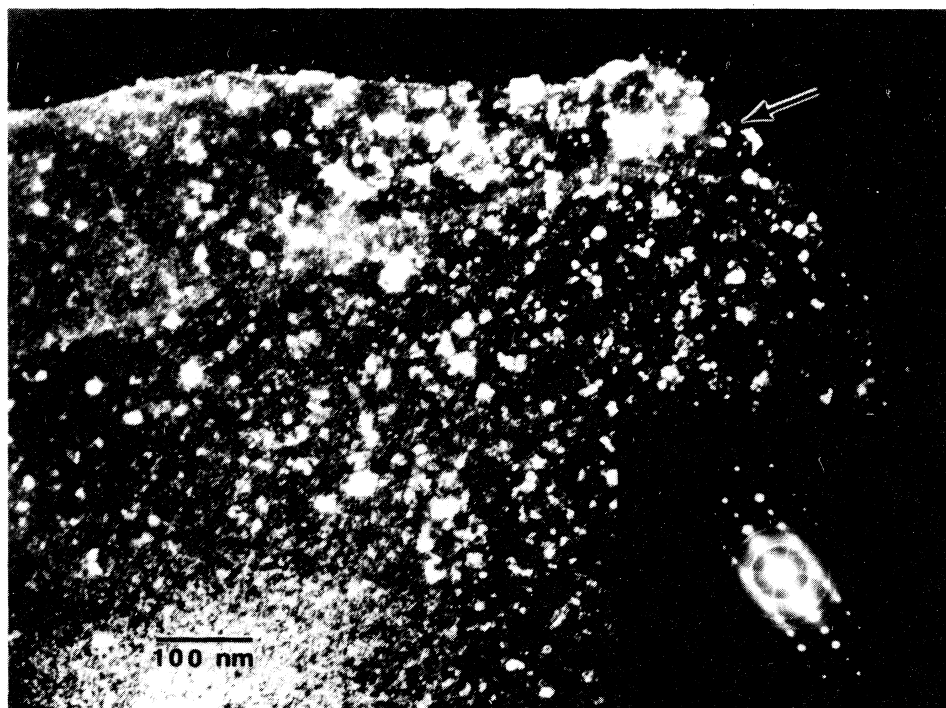


FIG. 2. Dark-field micrograph (formed predominantly from contributions of the diffracted beams due to the oxide phase) showing the  $\text{ZrO}_2$  precipitates. The distribution of the oxide phase does not appear to be significantly altered by the presence of the grain boundary (arrowed).

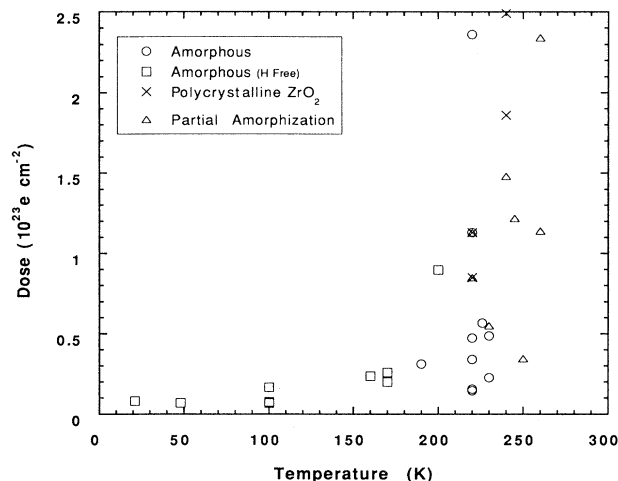


FIG. 3. The variation in the electron dose (electrons  $\text{cm}^{-2}$ ) required for amorphization for hydrogen-charged  $\text{Zr}_2\text{Ni}$  (cylindrical anode and gaseous charging). Complete amorphization ( $\circ$ ), partial amorphization ( $\triangle$ ), and formation of polycrystalline  $\text{ZrO}_2$  ( $\times$ ). Complete amorphization for the hydrogen-free  $\text{Zr}_2\text{Ni}$  ( $\square$ ).

temperature" is not due to changes in the electron dose rate (or beam heating effects); hydrogen-free material was irradiated at 220 K at significantly higher electron dose rates than the hydrogen-bearing alloy ( $\sim 7 \times 10^{19}$  compared to  $1.3 \times 10^{19}$  electrons  $\text{cm}^{-2} \text{s}^{-1}$  for the hydrogen-bearing material). Similarly, the differences in the total electron dose cannot account for the behavior; the hydrogen-free alloy was irradiated to a total dose of  $1.5 \times 10^{24}$  electrons  $\text{cm}^{-2}$  compared to as little as  $1.5 \times 10^{22}$  electrons  $\text{cm}^{-2}$  for complete amorphization of the hydrogen-bearing material. Despite an increase in the electron dose of more than two orders of magnitude and a higher dose rate, the uncharged  $\text{Zr}_2\text{Ni}$  did not undergo a transformation to the amorphous state at 220 K.

It is possible to provide some measure of the effect of dose rate and hydrogen content on the amorphization behavior of the alloys by normalizing the total dose required for amorphization by the dose rate and comparing this to the absolute hydrogen concentration. Such a comparison is shown in Fig. 4 for irradiations performed at 220 K. Those specimens which underwent complete amorphization are shown as open circles and the formation of the polycrystalline oxide phase is shown as a  $\times$ . The nominally hydrogen-free sample ( $< 0.4$  at. % H) exhibited no evidence for amorphization (but did show the formation of  $\text{ZrO}_2$ ) at this temperature. The data shown for the hydrogen-bearing alloys were obtained from those specimens cathodically charged using the cylindrical anode and via gas-phase charging. It can be seen from the figure that for hydrogen concentrations above 2 at. % the absolute hydrogen content and the dose rate produce no systematic variation in the amorphization behavior. Some variability in the electron dose required to produce complete amorphization is to be expected due to variations in the thickness of the irradiated region; however, it

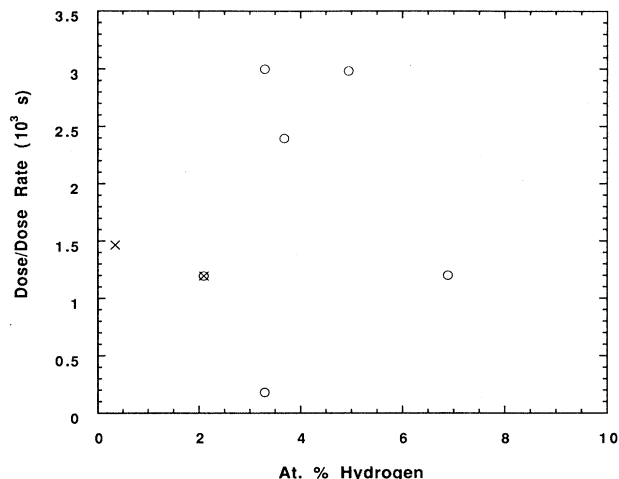


FIG. 4. The variation in the electron dose required for amorphization ( $\circ$ ), normalized by the dose rate, with the hydrogen content of the alloys at an irradiation temperature of 220 K. The formation of the oxide phase is marked by  $\times$ .

would seem improbable that this would mask any overall dependence on either the dose rate or the hydrogen content for the ranges examined. At a hydrogen concentration of 2 at. % some evidence for the formation of the polycrystalline oxide phase is found and this suggests, as will be discussed later, that this hydrogen content is close to the minimum for any enhancement of the amorphization behavior to be observed.

As noted previously, a number of specimens were electrochemically charged with hydrogen using a small plate anode. In this case the hydrogen, although equivalent in

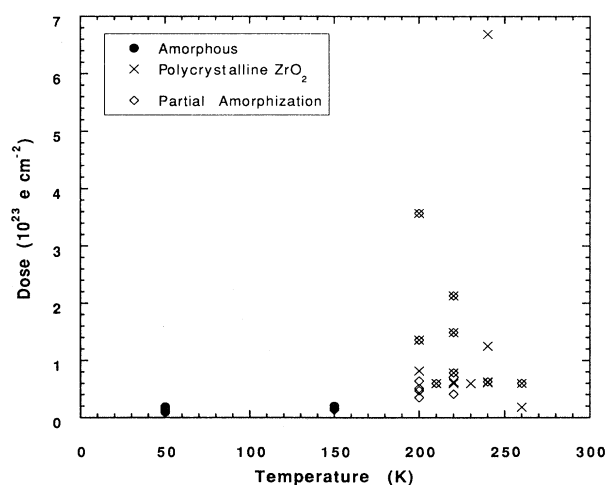


FIG. 5. The variation in the electron dose (electrons  $\text{cm}^{-2}$ ) required for amorphization for hydrogen-charged  $\text{Zr}_2\text{Ni}$  (plate anode). Total amorphization ( $\bullet$ ), partial amorphization ( $\diamond$ ), and the formation of polycrystalline  $\text{ZrO}_2$  ( $\times$ ). Note the change in the scale used for the electron dose compared to Figs. 1 and 3.

concentration to that obtained using the cylindrical anode, is expected to be concentrated predominantly on the face of the specimen which faced the anode. The significance of this alteration in the cathodic charging geometry can be seen in Fig. 5, where the variation in the electron dose required to produce amorphization with irradiation temperature is shown for  $Zr_2Ni$  specimens hydrogen charged on one face only. Below a temperature of 200 K the electron dose to amorphization is almost identical to that for the hydrogen-free material. Above 200 K there is only a slight indication that the amorphization behavior is enhanced, with some specimens exhibiting partial amorphization. None of the specimens, however, were observed to become completely amorphous at temperatures above 200 K despite the use of dose rates approaching  $1 \times 10^{20}$  electrons  $cm^{-2} s^{-1}$  and irradiation to much higher dose levels (note the change of scale in Fig. 5) than used to produce complete amorphization of the  $Zr_2Ni$  alloy charged with hydrogen on both faces (Fig. 3). In addition, in all cases, irradiation above 200 K produced the polycrystalline  $ZrO_2$  phase, a transformation which was only observed in a few isolated cases for those specimens charged with a cylindrical anode.

### B. $Zr_3Al$

Though less extensive than the  $Zr_2Ni$  data, the results for the  $Zr_3Al$  alloy showed qualitatively similar features. Nominally hydrogen-free  $Zr_3Al$  was irradiated at 22 and 30 K to a maximum dose of  $2.5 \times 10^{23}$  electrons  $cm^{-2}$ , equivalent to  $\sim 10$  displacements per atom. No amorphization was found at either temperature. Irradiation of the hydrogen-bearing (1.5 at. % H)  $Zr_3Al$  at 30 K was found to produce completely amorphous material at a dose of  $5.5 \times 10^{22}$  electrons  $cm^{-2}$  ( $\sim 2.2$  dpa). The irradiated areas showed no evidence for amorphization prior to irradiation, although other areas within the specimen were completely amorphous due to the presence of hydrogen. The large reduction in the electron dose required for amorphization of the hydrogen-bearing material is not due to dose rate effects, as a similar electron dose rate was used throughout. The formation of an oxide phase was not observed for either material.

## DISCUSSION

The data obtained for the variation in the electron dose required for amorphization with irradiation temperature for the hydrogen-free  $Zr_2Ni$  samples are generally consistent with those obtained by Xu *et al.*<sup>4</sup> in this system, and with molecular dynamics simulations.<sup>13</sup> The present study shows that on average the electron dose required for amorphization below 100 K is approximately  $7.6 \times 10^{21}$  electrons  $cm^{-2}$  ( $\sim 0.3$  dpa). Between 100 and 160 K the required dose increased to  $\sim 2.5 \times 10^{22}$  electrons  $cm^{-2}$  ( $\sim 1$  dpa). At 200 K, close to the "critical temperature," above which amorphization due to electron irradiation does not occur, the dose required for amorphization was approximately  $9 \times 10^{22}$  electrons  $cm^{-2}$ , which corresponds to  $\sim 3.5$  dpa. The data of Xu

*et al.*<sup>4</sup> are equivalent except at 160 K where the required electron dose was approximately 0.5 dpa. This reduction in dose appears to arise from the higher electron dose rate used by Xu *et al.*<sup>4</sup> [ $(1-2) \times 10^{-3}$  dpa  $s^{-1}$  compared to  $0.5 \times 10^{-3}$  dpa  $s^{-1}$  for the present study]. Similar dose rate effects have been observed for the CuTi (Ref. 14) and  $Zr_2(Fe,Ni)$  (Ref. 15) systems in the equivalent temperature range. The study by Xu *et al.*<sup>4</sup> also showed that an increase in the electron dose required for amorphization occurred at 110–120 K, which was attributed to the recovery of the damaged state by point-defect migration. Such an analysis is consistent with the effect of electron dose rate in this temperature range: a higher dose rate appears to allow a more rapid approach to the amorphous state when defect annealing is occurring. The influence of electron dose rate is found to be insignificant at low temperature, where recovery does not occur.

The formation of an oxide phase at temperatures above the "critical temperature" (above which amorphization does not occur) has not been reported previously for this alloy, to our knowledge, although Motta, Howe, and Okamoto<sup>16</sup> have reported a similar phase for the alloy  $Zr_3Fe$  as the "critical temperature" is approached. Calculations performed using the method of Fisher<sup>10</sup> suggest that it cannot be attributed to electron-beam heating effects, as the temperature rise, even at the highest dose rates examined ( $1 \times 10^{20}$  electrons  $cm^{-2} s^{-1}$ ,  $\Delta T \sim 45$  K), is insufficient to increase the temperature above 300 K, a temperature where no oxide formation was observed in the absence of irradiation. As noted previously, this oxide phase appears to form by reaction of Zr with trace oxygen in the TEM, rather than from internal oxygen contamination of the specimen. If this is correct, the facts that the oxide is not observed on even quite old specimens which have been stored at room temperature in air, and that it only forms within the area defined by the electron beam during irradiation, strongly suggest that it is due to segregation of Zr to the surface during irradiation. The surface is known to act as an efficient sink for interstitial atoms in thin-foil TEM specimens and the surface segregation of Zr would result if Zr forms a mobile interstitial which migrates to the surface. Alternatively, the Zr could form a stable complex with vacancies which migrate to the surface, resulting in solute (Zr) drag and Zr segregation at the surface.

The introduction of hydrogen by cathodically charging specimens of  $Zr_2Ni$  using a cylindrical anode, or by gas-phase charging, increased the upper temperature at which amorphization could be achieved to approximately 260 K (Fig. 3). This increase in the "critical temperature" may be due to a number of factors: an increase in the rate of Frenkel pair production, the formation of collision cascades, the direct amorphization by hydrogen, or the stabilization of the defect structure by the trapping of lattice defects by hydrogen.

An increase in Frenkel pair defect production can arise due to the presence of hydrogen. The presence of hydrogen solutes allows more effective energy transfer from the 1 MeV electrons to the lattice atoms via an intermediate hydrogen collision. The maximum energy transfer from a 1 MeV electron to a hydrogen atom, calculated using a

relativistic correction for the momentum of the electron,<sup>17</sup> is  $\sim 4.3$  keV compared to  $\sim 47$  eV for the energy transfer to the Zr atoms.

An increase in the "critical temperature" for amorphization has been observed when the mass of the bombarding particle is increased<sup>15,18</sup> due to the formation of displacement cascades. The possibility that displacement cascades are formed in the presence of hydrogen has been examined with calculations using the TRIM code,<sup>19</sup> which show that, even at much higher energies than would be realized with 1 MeV electrons, displacement cascades are not produced by electron irradiation via collisions with the hydrogen solutes. Consequently, the formation of displacement cascades is not expected, and has not been observed, indicating that the increase in the "critical temperature" is not the result of direct amorphization by collision cascades.

As discussed above, while increased efficiency in the formation of Frenkel pairs is expected in the presence of hydrogen, this does not appear to be the primary cause of the increase in the "critical temperature." This conclusion is supported by our observation that the increased "critical temperature" was not observed in specimens which were hydrogen charged on only one face, despite the fact that the average hydrogen concentration was the same as in specimens charged on both faces and that the presence of hydrogen did not significantly alter the electron dose required for complete amorphization at very low temperature (Fig. 5). In addition, Meng *et al.*<sup>2</sup> showed that the presence of a significantly higher hydrogen solute concentration only increased the efficiency of defect formation by about 40% (in  $Zr_3Al$  containing 24 at. % hydrogen). At 220 K, hydrogen-free  $Zr_2Ni$  did not exhibit amorphization even at doses as high as 59 dpa, while hydrogen-containing  $Zr_2Ni$  required only  $\sim 0.6$  dpa for complete amorphization. This factor of 100 is much larger than the  $\sim 1.4$  enhancement in defect production expected from the presence of hydrogen.

As an alternate explanation of the observations, we suggest that the primary effect of hydrogen is to stabilize the defect structure produced by electron irradiation of the  $Zr_2Ni$ . Solute hydrogen in  $Zr_2Ni$  does not cause amorphization by itself at hydrogen/metal ratios  $< 1.5$ ,<sup>5</sup> a concentration far higher than that examined in the present experiments. The presence of hydrogen can decrease the loss of point defects, due to diffusion to the external surfaces of the TEM specimens, by trapping the interstitial and/or the vacancy component of the damage. Several of the experimental observations support this hypothesis. An increase in the "critical temperature" is observed in specimens which have hydrogen introduced from both surfaces but not in specimens which were charged from only one surface. In the latter case, while the defect trapping slows diffusion towards the surface with the high hydrogen concentration, one of the specimen surfaces remains available as a sink for the defects produced by the irradiation. Additionally, the data shown in Fig. 4 indicate that there is no dose rate effect in the presence of hydrogen at an irradiation temperature of 220 K, consistent with the observation<sup>4</sup> that dose rate effects are observed only when the irradiation-induced de-

fects undergo annealing.

Additional evidence for this trapping effect is lent by the observations made on the formation of the  $ZrO_2$  at the surface of the specimens during irradiation. In the absence of irradiation, no  $ZrO_2$  formation was observed even for prolonged exposure to the atmosphere at 300 K. In the absence of hydrogen, the oxide was consistently observed during the irradiation (Fig. 1) above the "critical temperature" (200 K), consistent with defect-induced migration of Zr to the surface where it can oxidize. Below the "critical temperature" no oxide formation was observed, presumably because the Frenkel defects are retained in the structure and cause the observed amorphization. In contrast to this behavior, specimens containing hydrogen introduced from both surfaces (Fig. 3) generally do not exhibit  $ZrO_2$  formation even at temperatures well above the "critical temperature" for electron-irradiation-induced amorphization of the hydrogen-free  $Zr_2Ni$ . This is consistent with the trapping of the vacancies and interstitials by hydrogen, thus preventing their diffusion to the surfaces and the simultaneous drag of the Zr solute. When the hydrogen is introduced from one surface only (Fig. 5) the opposite surface remains a sink for the vacancies and interstitials, and, hence there is no increase in the "critical temperature" and solute drag occurs to that surface, resulting in formation of  $ZrO_2$  in all of the specimens irradiated above 200 K.

Formation of the  $ZrO_2$  occurs only in the irradiated areas under conditions where the surface can act as a sink for the point defects, consistent with solute drag by the diffusing point defects, or with Zr being the dominant interstitial defect. The absence of  $ZrO_2$  formation in specimens hydrogen charged from both surfaces is clear evidence for the trapping by hydrogen of the defects which cause Zr segregation at the surface.

The observed behavior is also consistent with experimental data for hydrogen diffusion in  $Zr_2Ni$ ,<sup>8,20</sup> which indicate that the onset of long-ranged diffusion occurs at temperatures between 250 and 290 K. This corresponds to temperatures above which hydrogen no longer appears to enhance the amorphization behavior; possibly because hydrogen can no longer effectively trap the defects when it becomes mobile.

Although harder to quantify than the  $Zr_2Ni$  data, the results obtained for the  $Zr_3Al$  system are qualitatively similar in many respects: the introduction of hydrogen into the alloy lattice during electropolishing significantly enhances the production of the amorphous phase by electron irradiation. The present study shows that, at 30 K, a hydrogen concentration of 1.5 at % reduces the electron dose required for complete amorphization to 2.2 dpa. Meng *et al.*<sup>1</sup> have reported similar findings: a hydrogen to metal atom ratio of 0.24 (24 at. %) decreased the electron dose required for amorphization at 10 K by a factor of more than 20: a dose of 26 dpa was required to produce approximately 90% amorphization of the hydrogen-free material, while complete amorphization was achieved at a dose of  $\sim 1$  dpa for the hydrogen-bearing alloy. The similarity in the electron dose required for amorphization in this study and in that of Meng *et al.*<sup>1</sup> (despite the large variation in the hydrogen

concentration) is consistent with the trapping of the point defects by hydrogen, as discussed for the  $Zr_2Ni$  data. The reduction in the electron dose required for amorphization for  $Zr_3Al$  due to the presence of hydrogen is substantial; a factor of about 26. As discussed above, this large effect is not consistent with the relatively small increase in the efficiency of Frenkel defect formation due to the presence of 24 at. % hydrogen; a factor of 1.4.

It is not possible to determine, from the present results, whether the presence of hydrogen reduces the dose to amorphization at temperatures well below the "critical temperature" for  $Zr_2Ni$ . However, the electron dose required for amorphization at 220 K for the hydrogen-bearing alloy is similar to that for the hydrogen-free material at 160 K, which suggests that the dose required for complete amorphization of the  $Zr_2Ni$  is relatively constant, except at temperatures close to the respective "critical temperatures." Such an interpretation is consistent with the proposition that the effect of hydrogen on amorphization is that it decreases the annealing of point defects in the temperature range where they would normally anneal out ( $T \sim 150\text{--}200$  K in hydrogen-free  $Zr_2Ni$ ).

In  $Zr_3Al$  hydrogen does appear to decrease the electron dose required for amorphization at 10 K, implying that point defects anneal out at this temperature. By analogy with the results for the  $Zr_2Ni$  system, this may indicate that this temperature (10 K) is close to the "critical temperature" for amorphization of  $Zr_3Al$ . Although appreciable recovery at such low temperatures appears rather anomalous, Koike *et al.*<sup>3</sup> noted the presence of defects within the irradiated microstructure of the hydrogen-free material at 10 K and suggest that such defects are indicative of point-defect motion, and hence recovery. Indeed the formation of such defects is not

normally noted in materials which become amorphous, and as noted by Meng *et al.*<sup>1</sup> were not observed in hydrogen-bearing  $Zr_3Al$  prior to amorphization, consistent with hydrogen trapping the point defects.

## CONCLUSIONS

We have examined the influence of hydrogen on the electron-irradiation-induced amorphization of  $Zr_2Ni$  and  $Zr_3Al$  and have shown that hydrogen solutes can significantly increase the upper temperature at which electron-irradiation-induced amorphization is possible. For irradiations performed at temperatures close to the "critical temperature" at which amorphization is possible in hydrogen-free material, the presence of hydrogen significantly reduces the dose required to produce complete amorphization. By altering the distribution of hydrogen in the  $Zr_2Ni$  specimens it has been shown that the primary role of hydrogen is to extend to higher temperatures the temperature range over which the point-defect population is stable. The results indicate that hydrogen acts to trap the point defects produced by electron damage in these intermetallic alloys.

## ACKNOWLEDGMENTS

This work was supported by the Department of Energy through Grant No. DEFG02-91ER45439 (University of Illinois). We would like to thank Dr. L. E. Rehn for the provision of the  $Zr_3Al$  and E. A. Ryan and S. Ockers of the Argonne National Laboratory for assistance in the operation of the HVEM. The use of the electron microscope facility in the Frederick Seitz Materials Research Laboratory is appreciated.

<sup>1</sup>W. J. Meng, J. Koike, P. R. Okamoto, and L. E. Rehn, in *Processing and Characterization of Materials using Ion Beams*, edited by J. E. Greene, L. E. Rehn, and F. A. Smidt, MRS Symposia Proceedings No. 128 (Materials Research Society, Pittsburgh, 1989), p. 345.

<sup>2</sup>W. J. Meng, P. R. Okamoto, L. J. Thompson, B. J. Kestel, and L. E. Rehn, *Appl. Phys. Lett.* **53**, 1820 (1988).

<sup>3</sup>J. Koike, P. R. Okamoto, L. E. Rehn, and M. Meshii, *Metall. Trans. A* **21**, 1799 (1990).

<sup>4</sup>G.-B. Xu, M. Meshii, P. R. Okamoto, and L. E. Rehn, *J. Alloys Compounds* **194**, 401 (1993).

<sup>5</sup>F. Aubertin, S. J. Campbell, and U. Gonser, *Hyperfine Interact.* **28**, 997 (1986).

<sup>6</sup>E. E. Havinga, H. Damsma, and P. Hokkeling, *J. Less-Common Met.* **27**, 169 (1972).

<sup>7</sup>T. Schober and D. G. Westlake, *Metallography* **14**, 359 (1981).

<sup>8</sup>F. Aubertin, S. J. Campbell, J. M. Pope, and U. Bonser, *J. Less-Common Met.* **129**, 297 (1987).

<sup>9</sup>A. Taylor, C. W. Allen, and E. A. Ryan, *Nucl. Instrum. Methods Phys. Res. Sect. B* **24/25**, 598 (1987).

<sup>10</sup>S. B. Fisher, *Radiat. Eff.* **5**, 239 (1970).

<sup>11</sup>T. C. Lee, D. K. Dewald, J. A. Eades, I. M. Robertson, and H. K. Birnbaum, *Rev. Sci. Instrum.* **62**, 1438 (1991).

<sup>12</sup>M. V. Nevitt, J. W. Downey, and R. A. Morris, *Trans. Metall. Soc. AIME* **218**, 1019 (1960).

<sup>13</sup>R. Devanathan, N. Q. Lam, P. R. Okamoto, M. J. Sabochick, and M. Meshii, *Phys. Rev. B* **48**, 42 (1993).

<sup>14</sup>J. Koike, D. E. Luzzi, M. Meshii, and P. R. Okamoto, in *Beam-Solid Interactions and Transient Processes*, edited by M. O. Thompson, S. T. Picraux, and J. S. Williams, MRS Symposia Proceedings No. 74 (Materials Research Society, Pittsburgh, 1987), p. 425.

<sup>15</sup>A. T. Motta, F. Lefebvre, and C. Lemaignan, in *Zirconium in the Nuclear Industry*, edited by C. M. Eucken and A. M. Garde, ASTM Special Technical Publication Vol. 1132 (American Society for Testing Materials, Philadelphia, 1991), p. 718.

<sup>16</sup>A. T. Motta, L. M. Howe, and P. R. Okamoto, *J. Nucl. Mater.* **205**, 258 (1993).

<sup>17</sup>D. R. Olander, *Aspects of Nuclear Fuel Elements* (Technical Information Center, Office of Public Affairs, Energy Research and Development Administration, Oak Ridge, TN, 1976).

<sup>18</sup>J. Koike, P. R. Okamoto, L. E. Rehn, and M. J. Meshii, *J. Mater. Res.* **4**, 1143 (1989).

<sup>19</sup>J. F. Ziegler, J. P. Biersack, and U. Littmark, in *The Stopping and Range of Ions in Solids*, edited by J. F. Ziegler (Pergamon, New York, 1985).

<sup>20</sup>A. Baudry, P. Boyer, and A. Chickdene, *J. Less-Common Met.* **143**, 143 (1988).

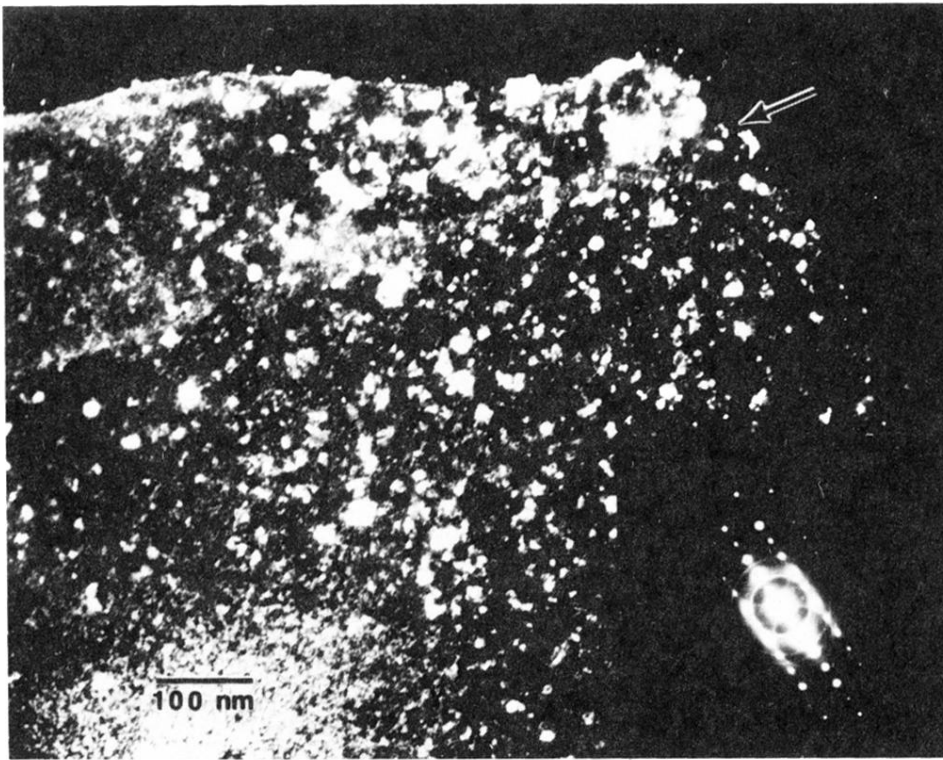


FIG. 2. Dark-field micrograph (formed predominantly from contributions of the diffracted beams due to the oxide phase) showing the  $ZrO_2$  precipitates. The distribution of the oxide phase does not appear to be significantly altered by the presence of the grain boundary (arrowed).